# Joining of High Strength Low Ductility AA7055 by Friction Self-piercing Rivet

Yong Chae Lim*, Hui Huang, Yiyu Wang, Yuan Li, Zhili Feng

[1]Materials Science & Technology Division, Oak Ridge National Laboratory, One Bethel Valley Road, Oak Ridge, TN 37831, USA
(limy@ornl.gov, huangh@ornl.gov, wangy4@ornl.gov, liy5@ornl.gov, fengz@ornl.gov)

*Corresponding author: Dr. Yong Chae Lim (limy@ornl.gov)
Tel: +1-865-574-4805
Address: One Bethel Valley Road, Oak Ridge, TN 37831, USA

Keywords: Friction self-piercing riveting; High strength 7xxx Aluminum alloys; Mechanical joint properties; Solid-state joining

## ABSTRACT

High strength aluminum (Al) alloy is one of higher specific strength materials for decarbonization in transportation industries. Because of low ductility at room temperature, conventional mechanical fastening such as self-piercing riveting produces cracks at the joint. In this work, we applied friction self-piercing riveting to join Al alloy (AA) 7055. No cracks were observed in the joints because of the improved local ductility of Al alloy by the generated frictional heat during joining step. Numerical modeling of joining process was applied to guide rivet geometry design and rivet material strength. Mechanical integrity of the AA7055 joints was assessed by lap shear tensile and cross-tension testing. Metallurgical characterizations revealed solid-state bonding formed not only between the rivet and surround Al materials, but also upper and lower Al sheets at the joint interface. Both solid-state bonding and mechanical interlocking between the flared rivet and bottom AA7055 sheet were the major joint mechanisms.

# 1 Introduction

High strength aluminum alloy (AA) is considered as a one of higher specific strength materials for lightweight vehicle applications. 7xxx AA (Al-Zn-Mg-Cu) has much higher strength than the 5xxx and 6xxx Al alloys, leading to great potential for decarbonization in vehicle applications. One of technical obstacle to prevent widespread of 7xxx AA for transportations is lack of suitable joining process. For example, fusion welding of 7xxx AA shows a solidification cracking because of different solidification rates between copper-rich zone and copper-free zone [1]. Another example is a cold cracking problem when mechanical fastening (e.g., self-piercing riveting (SPR)) is used at room temperature [2]. This is mainly due to low ductility at room temperature. Therefore, additional auxiliary heating system and joining step are required, increasing joining process time and cost.

To alleviate the above issues, solid-state based joining processes, such as friction stir welding (FSW) or refill friction stir spot welding were used for joining of 7xxx Al alloy by avoiding melting of material with relatively low heat input compared with conventional fusion welding [3,4]. However, strength loss in the thermomechanical affected zone and heat affected zone (HAZ) is a still problem. Recently, friction based self-piercing riveting process is developed for joining of low ductility lightweight materials such as magnesium alloy, 7xxx AA, and carbon fiber reinforced composites without cracking issue [5,6,7,8,9,10].

In this work, we applied F-SPR process to join AA7055-T76 to AA7055-T76 by varying process conditions such as spindle rotational speeds and axial plunge depths. Mechanical joint strength of F-SPR joints was evaluated by lap shear tensile testing. Cross-sectional analysis for F-SPR joint was conducted to study joint formation. Vickers microhardness measurement was used to assess the local hardness evolution due to frictional heat and shear stress during F-SPR process.

# 2. Materials and experimental methods

## 2.1. Materials

In this work, 2.5 mm thickness of high strength AA 7055-T76 sheets were used to spot join by F-SPR process. Chemical compositions and mechanical properties of the AA7055-T76 are summarized in Table 1 and Table 2. For a consumable rivet, 1018 low carbon steel was employed to fabricate the hexagonally designed rivet head (9.535 mm width) to be externally driven by the tool holder during joining process. The rivet diameter (6.8 mm) and leg length (6 mm) were customized for the selected Al alloy. For back supporting anvil, a flat die with 1.5 mm cavity depth was used to induce material flow and produce mechanical interlocking between the rivet and bottom Al sheet.

Table 1. Summary of chemical composition of AA7075-T76 [11].

| Element (wt%) | Zn | Mg | Cu | Zr | Cr | Si | Fe | Mn | Ti | OE | OT | Remainder |
|---|---|---|---|---|---|---|---|---|---|---|---|---|
| AA7055-T76 | 7.6~ 8.4 | 1.8~ 2.3 | 2.0~ 2.6 | 0.08~ 0.25 | 0.04 max | 0.10 max | 0.15 max | 0.05 max | 0.06 max | 0.05 max | 0.15 max | Al |

Table 2. Material properties of AA7055-T76 [11].

| Material properties | Yield strength (MPa) | Tensile strength (MPa) | Elongation (%) |
|---|---|---|---|
| AA7055-T76 | 586 | 613.6 | 7 |

AA7055 sheets were cut into lap shear coupons (40 mm wide and 120 mm long), as depicted in Figure 1. Al surfaces were cleaned by acetone to remove any greases and dusts before joining.

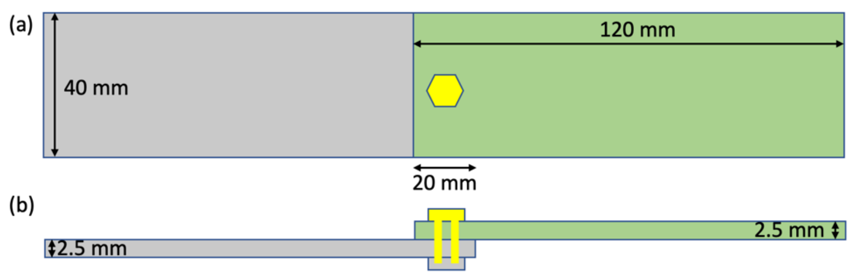


Figure 1. A schematic of lap shear tensile coupon. (a) Top view, (b) side view.

## 2.2. Description of F-SPR process

A description of the F-SPR process can be found in the authors' prior publications [9,10]. A brief explanation of the joining process is provided for readers. As illustrated in Figure 2, a spinning rivet with an axial downward force is plunged into stacked Al sheets. During this step, local frictional heat is produced between the rivet and the bottom Al sheet metal, resulting in improved local ductility of the AA7055-T76. Finally, the rivet leg flares out in the bottom Al sheet based on the supporting die geometry, leading to mechanical interlocking in the workpiece. F-SPR process was initially developed by varying spindle rotation speeds and axial plunge depths at fixed axial plunge speed of 2.86 mm $s^{-1}$ that is a maximum speed of the current our joining machine. The F-SPR process conditions were optimized by achieving the highest lap shear fracture load and no cracking on the backside of the AA7055-T76.

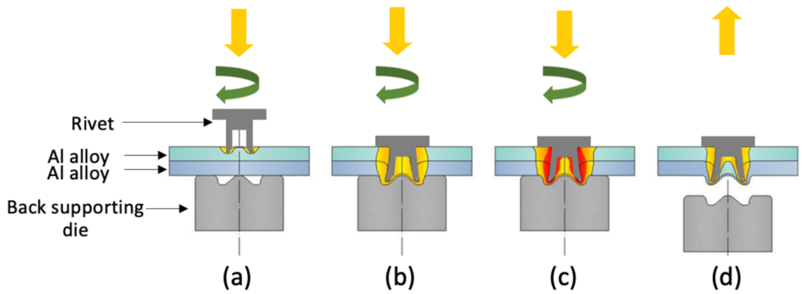


Figure 2. A schematic of F-SPR process.

2.3. Description of lap shear tensile testing

Lap shear tensile testing was conducted to assess the joint strength of F-SPR specimens by an MTS Systems tensile machine with a constant crosshead speed of 10 mm $min^{-1}$ at room temperature. Spacers were used to hold the lap shear coupons to align them vertically between the grips during lap shear tensile testing.

2.4. Metallography characterizations

The joint formation between the rivet and Al sheet was characterized by the cross-sectioned F-SPR coupon. The sample was cross-sectioned, mounted, grinded, and polished for metallographic characterization using standard metallographic processes. Then, an optical microscope was used to measure characteristic length of the joint and any metallurgical bonding during joining process. A microhardness tester (Leco LM 100AT) was used for Vickers microhardness measurement. Each welded sample was tested under following conditions: 200 µm spacing, 100 g of load, and 13 seconds of dwell time.

**3. Results and discussion**

3.1. Lap shear tensile strength of F-SPR joints

Load versus displacement curves from lap shear tensile testing are plotted in Figure 3. The average peak failure load was found to be 11.70 ± 0.17 kN. Displacement at failure is ranged from 6 mm to 6.6 mm, indicating more ductile failure than the brittle mode. Figure 4 shows representative fractographic image from lap shear tensile testing of F-SPR joint. The rivet pulled out the bottom sheet of AA7055-T76, as shown in Figure 4(a). Cavity in the rivet was filled with upper and lower sheet of Al alloy. Also, some Al materials retained at the periphery of the rivet after lap shear tensile testing, resulting in partial Al sheet fracture at the periphery of the joint. The strong mechanical joint strength can be attributed not only to the mechanical interlocking of the flared rivet with the bottom aluminum sheet, but also to the solid-state joining of the rivet with the surrounding aluminum sheet. Further metallurgical characterizations were performed to study the joint mechanism in the next section.

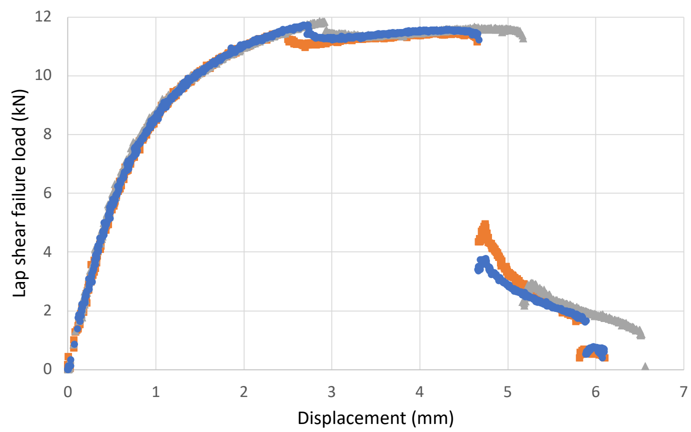


Figure 3. Load and displacement curves for lap shear tensile tested F-SPR AA7055-T76 joints.

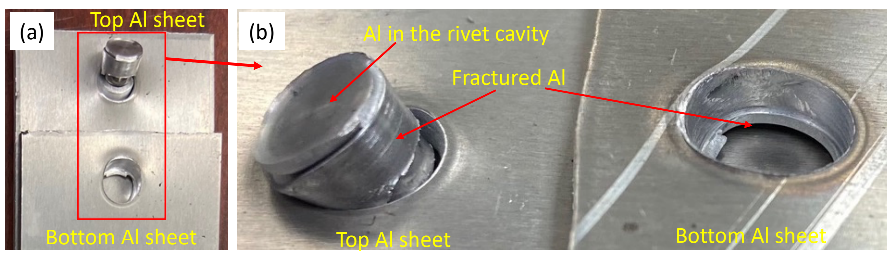


Figure 4. (a) Fractured F-SPR joints after lab shear tensile testing. (b) magnified fractography, showing Al pullout failure mode.

3.2. Metallurgical characterizations

Figure 5 provides a cross-sectional view of the F-SPR Al joint. Mechanical interlocking distance (two red lines on each side) was measured as 0.4 mm. Mechanical interlocking size determines the level of locking strength between the rivet and the bottom sheet, along with the load path within the joint. Friction heat generated during F-SPR improves local ductility of Al alloy, so no cracking of AA7055 was observed in Figure 5(a). It is found out that ductility of AA7075-T6 is increased at temperature ranged from 150°C to 250°C [12]. In addition, Ying et al applied thermal assisted SPR for AA7075-T6 [13]. Maximum mechanical joint strength was achieved without crack on the Al alloy when temperature is ranged from 400 to 450°C. Figure 5(b) and (c) show a solid-state bonding between upper Al and lower Al sheets at both left (red dot circle) and right sides caused by the frictional and downward axial force. Measured solid-state joining size is approximated 30 μm. Also, F-SPR process induces Al material flow near the joint interface, forming a hook shape. Next, grain refinement of Al near the joint is seen due to dynamic recrystallization. Figure 5(d) presents a solid-state bonding between upper and lower Al sheet at the rivet cavity. This solid-state joining is facilitated by spinning motion of rivet under frictional heat and compression load during F-SPR process. Figure 5(e) shows grain refinement of upper Al sheets where solid-state joining has taken place with lower Al sheets. Finally, material flow and grain refinement at the rivet tip is presented in Figure 5(f). Again, plastic deformation of lower Al sheet under large shear motion and frictional heat during F-SPR induces such material flow and refinement of grain in the lower Al sheet.

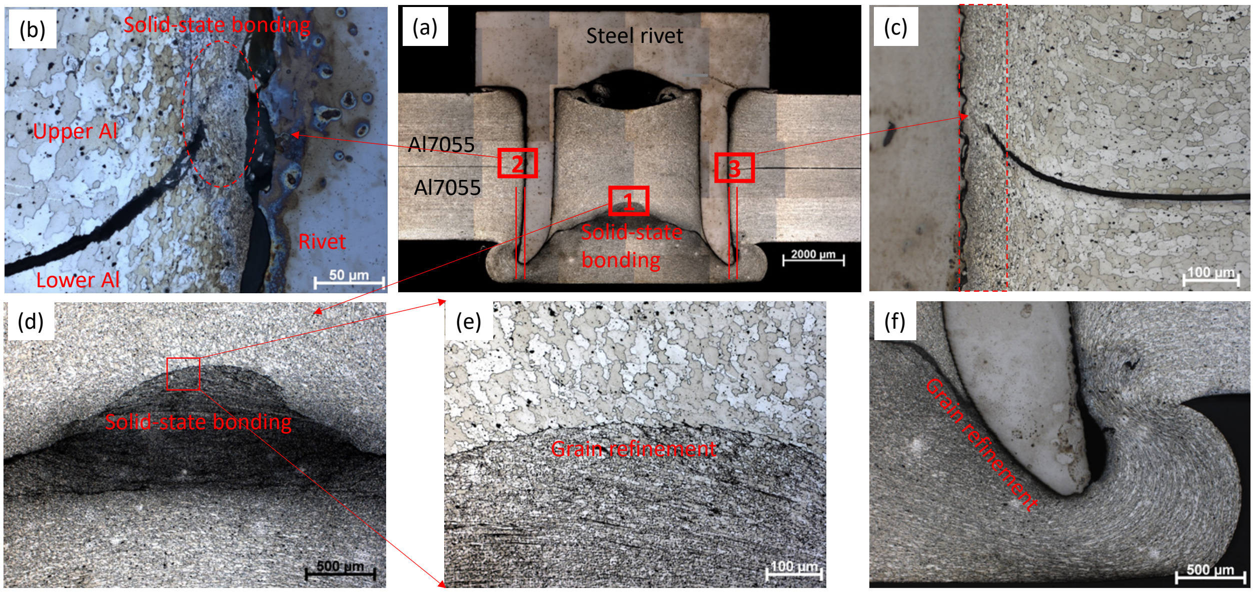


Figure 5. Optical image of cross-sectioned F-SPR AA7055 joint at different joint locations. (a) Low magnification optical image, showing mechanical interlocking between the rivet and bottom Al sheet. No cracking of bottom Al sheet was observed. (b) Magnified optical image at left side joint interface, showing solid-state bonding between upper and lower Al sheets (red dot circle). (c) Magnified optical image at the right side joint interface, showing grain refinement of Al sheets near joint interface (red dot box). (d) Solid-state joining between upper and lower Al sheets at the rivet cavity. (e) magnified optical image showing grain refinement. (f) grain refinement of Al and material flow at the right side rivet tip.

Vickers microhardness mapping of steel rivet and AA7055-T76 in the F-SPR joint is presented in Figure 6(a). The line scans (two dot blacklines) of the steel rivet and Al alloy where Y=4 mm and 2.6 mm are plotted in Figure 6(b). The average Vickers microhardness of steel rivet is approximately 280HV. There is no significant reduction of hardness for the steel shank because frictional heat did not cause high temperature to soften the steel rivet. From open literature, it is found that mechanical properties (i.e., yield and tensile strength) for low carbon steel (ASTM 1022) starts reducing above 400 ºC [14]. Therefore, it is rational that estimated peak temperature during F-SPR is less than 400 ºC.

The Vickers microhardness of as-received AA7055-T76 is measured to be ranged from 180 to 195HV. The microhardness of AA7055-T76 near the steel rivet-Al alloy joint interface is about 230HV which is much higher than the base material. This higher hardness results from the grain refinement caused by dynamic recrystallization during F-SPR process, as shown in Figure 6(c) [red dot box]. Refined grain zone is approximately 130 µm. Above this distance, there is a local reduction of microhardness caused by frictional heat during F-SPR. This soft zone is about 2 mm long. Then, microhardness is back to the 180~195HV again. This local hardness drop zone (i.e., HAZ) can be corelated to the fracture location of F-SPR joints from lap shear tensile testing. Estimated peak temperature below 400 ºC is not only high enough to increase local ductility to avoid cold crack, but also to induce local hardness drop at the joint location. For this reason, weakest location is at the HAZ based on the current F-SPR joint process parameters.

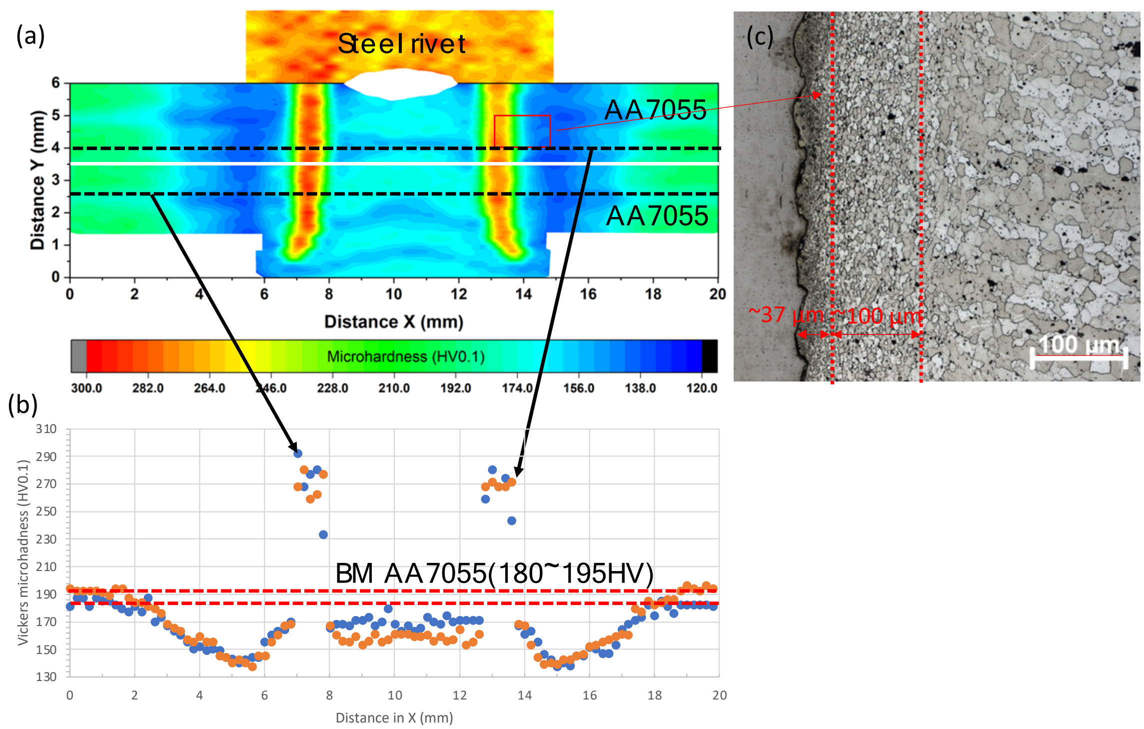


Figure 6. (a) mapped Vickers microhardness measurement for F-SPR Al joint. (b) line plotted Vickers microhardness at Y distance= 4 mm and 2.6 mm in (a). (c) Optical micrograph at the right side joint, showing grain size gradient. Refined grain near the joint interface was found, and then grain size increased as moved toward to right direction.

## 4. Conclusions

F-SPR process was developed to spot join high strength low ductility AA7055-T76. Frictional heat generated during F-SPR process improved local ductility of Al alloy, resulting in crack free joint. The averaged lap shear fracture load is 11.7 kN with failure of the bottom Al sheet, indicating strong mechanical interlocking between the flared rivet and bottom Al sheet. From the cross-section characterization, solid-state joining between upper Al and lower Al sheet at the joint interface was found. Due to frictional heat and high shear motion, grain refinement of Al alloy near the joint interface was also observed. Vickers microhardness measurement reveals the local hardness drop of Al alloy near the joint due to frictional heat during F-SPR.


## Acknowledgements

The authors would like to acknowledge the financial support of the U.S. Department of Energy Office of Energy Efficiency and Renewable Energy, Vehicle Technology Office, as part of Joining Core Program. Oak Ridge National Laboratory is managed by UT-Battelle, LLC for the U.S. Department of Energy under Contract DE-AC05-00OR22725. The authors thank to Russell Long at Arconics providing materials.

## Reference

[1] Temmar M, Hadji M, Sahraoui T (2011) Effect of post-weld aging treatment on mechanical properties of tungsten inert gas welded low thickness 7075 aluminium alloy. Joints Mater. Des. 32(6):3532–3536.
[2] Jäckel M, Grimm T, Landgrebe D (2016) Approaches for mechanical joining of 7xxx series aluminum alloys. AIP Conf. Proc. 1769:100010.
[3] Rajakumar S, Muralidharan C, Balasubramanian V (2011) Influence of friction stir welding process and tool parameters on strength properties of AA7075-T6 aluminium alloy joints. Mater. Des. 32(2):535–549.
[4] Shen Z, Yang X, Zhang Z, Cui L, Li T (2013) Microstructure and failure mechanisms of refill friction stir spot welded 7075-T6 aluminum alloy joints. Mater. Des. 44:476–486.
[5] Li Y, Wei Z, Wang Z, Li Y (2013) Friction self-piercing riveting of aluminum alloy AA6061-T6 to magnesium alloy AZ31B. J. Manuf. Sci. Eng., 135(6):061007.
[6] Liu X, Lim YC, Li Y, Tang W, Ma Y, Feng Z, Ni J (2016) Effects of process parameters on friction self-piercing riveting of dissimilar materials. J. Mater. Proc. Technol. 237:19–30.
[7] Lim YC, Warren CD, Chen J, Feng Z (2019) Joining of lightweight dissimilar materials by friction self-piercing riveting
[8] Ma YW, Li YB, Lin ZQ (2019) Joint formation and mechanical performance of friction self-piercing riveted aluminum alloy AA7075-T6 joints. J. Manuf. Sci. Eng. 141:041005.
[9] Lim YC, Chen J, Jun J, Leonard D, Brady MP, Warren CD, Feng Z (2021) Mechanical and corrosion assessment of friction self-piercing rivet joint of carbon fiber-reinforced polymer and magnesium alloy AZ31B. J. Manuf. Sci. Eng. 143(3):031006.
[10] Lim YC, Jun J, Leonard D, Li Y, Chen J, Brady MP, Feng Z (2022) Study of galvanic corrosion and mechanical joint properties of AZ31B and carbon-fiber-reinforced polymer joined by friction self-piercing riveting. J. Magnes. Alloy. 10(2):400-410.
[11] Alcoa aerospace technical fact sheet “Alloy 7055-T74511 and 7055-T76511 extrusions.”
[12] Huo W, Hou L, Zhang Y, Zhang J (2016) Warm formability and post-forming microstructure/property of high-strength AA 7075-T6 alloy. Mater. Sci. Eng. A. 675:44-54.
[13] Ying L, Gao T, Dai M, Hi P, Dai J (2021) Towards joinability of thermal self-piercing riveting for AA7075-T6 aluminum alloy sheets under quasi-static loading conditions. Int. J. Mech. Sci. 189:105978.
[14] Nikulin SA, Rogachev SO, Nikolaev YA, Vasiliev SG, Belov VA, Turilina VY (2021) High-temperature mechanical properties of low-carbon steel used for the manufacture of core catcher vessel. Prog. Nucl. Energy 142:104015.